Contents lists available at SciVerse ScienceDirect

Analytical Biochemistry

journal homepage: www.elsevier.com/locate/yabio

# Electrochemical titrations and reaction time courses monitored in situ by magnetic circular dichroism spectroscopy

Justin M. Bradley [a], Julea N. Butt [a,b,*], Myles R. Cheesman [a,*]

[a] Centre for Molecular and Structural Biochemistry, School of Chemistry, University of East Anglia, Norwich Research Park, Norwich NR4 7TJ, UK
[b] Centre for Molecular and Structural Biochemistry, School of Biological Sciences, University of East Anglia, Norwich Research Park, Norwich NR4 7TJ, UK

ARTICLE INFO

*Article history:*
Received 23 April 2011
Received in revised form 24 July 2011
Accepted 25 July 2011
Available online 30 July 2011

*Keywords:*
MCD
Magnetic circular dichroism
Electrochemistry
Metalloprotein

ABSTRACT

Magnetic circular dichroism (MCD) spectra, at ultraviolet–visible or near-infrared wavelengths (185–2000 nm), contain the same transitions observed in conventional absorbance spectroscopy, but their bisignate nature and more stringent selection rules provide greatly enhanced resolution. Thus, they have proved to be invaluable in the study of many transition metal-containing proteins. For mainly technical reasons, MCD has been limited almost exclusively to the measurement of static samples. But the ability to employ the resolving power of MCD to follow changes at transition metal sites would be a potentially significant advance. We describe here the development of a cuvette holder that allows reagent injection and sample mixing within the 50-mm-diameter ambient temperature bore of an energized superconducting solenoid. This has allowed us, for the first time, to monitor time-resolved MCD resulting from in situ chemical manipulation of a metalloprotein sample. Furthermore, we report the parallel development of an electrochemical cell using a three-electrode configuration with physically separated working and counter electrodes, allowing true potentiometric titration to be performed within the bore of the MCD solenoid.



Magnetic circular dichroism (MCD)[1] spectroscopy, at ultraviolet–visible and near-infrared wavelengths (185–2000 nm), has proved to be invaluable in the study of metalloproteins containing cofactors such as heme [1–3], non-heme iron [4], iron–sulfur clusters [5–8], cobalt [9,10], nickel [11–13], and copper [14,15]. The technique measures the apparent circular dichroism (CD) induced by a magnetic field [16]. Despite similarities in the instrumentation used, the observation of MCD is not dependent on the chirality of the protein; the method is equally applicable to racemic model complexes [17]. The magnetic field will always induce signals across wavelengths at which the substance absorbs. Thus, MCD spectra contain the same electronic transitions observed in conventional absorbance spectroscopy, but the bisignate nature of the spectrum provides enhanced resolution and greater detail. This spectral detail offers an unmatched fingerprinting capability that can, for example, identify the spin and oxidation states of heme groups [1] and distinguish among the variety of iron–sulfur centers found in biological molecules [18–20].

Metalloprotein MCD can be measured at ambient or cryogenic temperatures. The latter requires adulteration with glassing agents [16] but has generally been preferred because MCD intensity from paramagnetic centers increases dramatically at low temperature. Thus, most metalloprotein MCD reported has been measured in glasses at temperatures of approximately 4.2 K. Hemoproteins represent the significant exception, giving rise to appreciable MCD at high temperatures [1]. Thus, ambient temperature MCD is used to diagnose spin state, oxidation state, and (in the case of low-spin Fe(III) hemes) axial ligation [21].

As with many techniques, much valuable information is to be gained from the ability to follow spectral perturbations that report on changes at the metal center. This includes equilibrium studies (chemical or redox titrations) as well as kinetic measurements. For technical reasons, such use of MCD has been limited almost exclusively to the measurement of series of static samples. Limited time domain studies have been achieved using a freeze–quench approach; samples can be frozen in approximately 30 s after preparation [22,23]. Alternatively, reacting aqueous samples can be quenched in cold liquids such as isopentane and, with considerable effort, packed into quartz tubes for electron paramagnetic resonance (EPR) [24]. However, this method presents additional challenges for MCD because achieving an optically transparent

* Corresponding authors. Fax: +44 1603 592003.
*E-mail addresses:* j.butt@uea.ac.uk (J.N. Butt), m.cheesman@uea.ac.uk (M.R. Cheesman).

[1] *Abbreviations used:* MCD, magnetic circular dichroism; CD, circular dichroism; MOTTLE, MCD-monitored optically transparent thin layer electrochemistry; T, Tesla; RT, room temperature; $cd_1$, cytochrome $cd_1$; Paz, pseudoazurin; $Tyr^-$, tyrosinate; SHE, standard hydrogen electrode.

0003-2697/$ - see front matter © 2011 Elsevier Inc. All rights reserved.
doi:10.1016/j.ab.2011.07.030

sample requires mixing with glycerol at −30 °C to form a slurry. Although these multiple-sample methods can be used to chart changes at metal sites by MCD, they suffer from significant disadvantages. Large amounts of material are consumed, and they are extremely low throughput with, at best, two or three samples processed per day. Thus, it is difficult to monitor time-dependent events with useful resolution.

Similar problems beset MCD-monitored redox titrations. Multiple samples can be electrochemically poised and frozen for measurements. But again sample consumption is high, throughput is low, and drifts in potential can occur during the freezing process. We previously developed a method by which MCD could be used to probe the nature of a metalloprotein sample poised in situ at defined electrochemical potential [25]. The method, MCD-monitored optically transparent thin layer electrochemistry (MOTTLE), uses a three-electrode cell in a quartz cuvette, including an optically transparent working electrode. The shortest dimension of the cell by far is in the direction of the light path (0.5–1.0 mm). Diffusion allows the sample to come to pseudo-equilibrium with applied potential because the distance between transparent faces of the cell and the working electrode (0.25–0.5 mm) is far shorter than the separation of working and counter electrodes (~5.0 mm). This configuration of MOTTLE has already made significant contributions to the understanding of hemoproteins, especially those containing multiple cofactors [26,27].

The ability to use ambient temperature MCD to follow reactions initiated by in situ mixing of reagents would represent a significant advance. This requires reagent injection lines and a non-magnetic stirring mechanism sited inside the bore of a superconducting solenoid. A stirring mechanism would also require larger volume and longer pathlength cuvettes. However, this is also a prerequisite for physical separation of counter and working electrodes, a modification of MOTTLE that would allow true equilibrium to be reached at times minimized by the stirring. Longer pathlengths, especially if combined with stronger magnetic fields, would also increase MCD signal magnitude, facilitating the study of cofactors other than heme.

Such developments have previously been precluded by the solenoid bore diameter (25 mm). Stirring and injection mechanisms cannot be constructed in this limited space. Consequently, we have commissioned a superconducting solenoid that gives magnetic fields of up to 8 Tesla (T) and is fitted with a room temperature (RT) bore of 50 mm diameter. We report here the design, construction, and performance of apparatus that allows realization of the twin aims of in situ triggering of reactions followed by time-resolved RT MCD and enhanced potentiometric performance with stirred electrochemical cells.

## Materials and methods

MCD spectra were recorded using a Jasco J-810 spectropolarimeter with the sample located in an 8-T magnetic field within the ambient temperature bore of an Oxford Instruments Special Spectromag 1000 superconducting solenoid. Absorbance spectra were recorded using a Hitachi U-2900 spectrometer. All potentiometric and voltammetric measurements were performed using an Autolab PGSTAT12 instrument controlled by GPES software. Calibration of the Ag/AgCl reference electrode was as described previously [25].

### *Redox cycling of Paracoccus pantotrophus $cd_1$*

Cytochrome $cd_1$ ($cd_1$) was expressed and purified using established protocols [28]. Protein concentration was determined by electronic absorbance spectroscopy of the oxidized form using $\varepsilon_{406\ nm}$ = 143,000 $M^{-1}$ $cm^{-1}$ per monomeric unit [29]. In situ injection of aliquots of reagent into a cuvette positioned in the bore of the superconducting solenoid was achieved using flexible cannulas. These were loaded with anaerobic reagents while in an $N_2$-filled chamber ($O_2$ < 5 ppm). Aliquots of reagent were loaded into the cannulas from a gas-tight syringe and were alternated with 5-μl aliquots of buffer. Sufficient nitrogen gas was drawn into the cannulas between reagent aliquots such that depression of the plunger to expel a total of 50 μl of gas and liquid from the barrel would deliver an accurately known volume (typically 1–3 μl) of reagent into the MCD cell. Cannulas were threaded through access channels in a purpose-built cuvette holder, and the tips were introduced into the cuvette through a Teflon lid (apparatus described below). The entire assembly was then removed from the $N_2$ chamber and immediately inserted into the bore of the solenoid. Insertion of a cannula provided a continuous flow of $N_2$ gas (humidified to prevent evaporation from sample) to drive a stirring mechanism and to remove dioxygen from the bore. Any trace oxygen inadvertently introduced during transfer was removed by stirring the sample under a flow of $N_2$ while the solenoid was charged (~10 min). The dimensions of the cell holder and cannulas were such that, once in place in the magnet bore, the entire length of the injection lines containing reagent were located within the region purged with nitrogen gas to maintain their anaerobicity.

### *Potentiometry of P. pantotrophus pseudoazurin and horse heart cytochrome c*

Horse heart cytochrome *c* (Acros Organics) was used without further purification. Concentrations were determined by electronic absorbance spectroscopy using $\varepsilon_{410}$ = 106,100 $M^{-1}$ $cm^{-1}$ for the Fe(III) state [30]. MCD-monitored potentiometric titrations were performed on cytochrome *c* samples of 6 μM concentration in 20 mM Hepes and 50 mM KCl (pH 7.4) containing the following mediators (each at 4 μM concentration): potassium ferricyanide, phenazine methosulfate, tetramethyl-*p*-phenylene diamine, anthraquinone-2,6-disulfonic acid, 2-anthraquinone sulfonic acid, 2-methyl-1,4-naphthoquinone, and tetramethyl-*p*-benzoquinone. Pseudoazurin (Paz) from *P. pantotrophus* was obtained as a by-product of the purification of $cd_1$ [28].

Concentrations were determined by electronic absorbance spectroscopy of the oxidized form using $\varepsilon_{590nm}$ = 3000 $M^{-1}$ $cm^{-1}$ [31]. CD-monitored potentiometric titrations with Paz were performed on samples of 50 μM concentration in 50 mM potassium phosphate and 50 mM KCl (pH 8.0) and the following mediators (each at 4 μM concentration): potassium ferricyanide, phenazine methosulfate, tetramethyl-*p*-phenylene diamine, methyl-1,4-naphthoquinone, and tetramethyl-*p*-benzoquinone.

For both CD- and MCD-monitored potentiometric titrations, the sample was equilibrated at a set potential until both the spectral response at a fixed wavelength (550 nm for cytochrome *c* and 470 nm for Paz) and the current flowing in the cell became invariant with time. A full-wavelength scan was then recorded while monitoring the stability of the potential in the cell using the galvanostat mode of the Autolab PGSTAT.

## Results

### *Construction of cell assembly*

The apparatus was designed to position variable-pathlength cuvettes in the center of the solenoid, incorporating reagent delivery and stirring mechanisms while maintaining the bore anaerobic. For operation in the bore of the solenoid, the stirring mechanism must be metal free. A system for stirring cuvettes of 10 mm

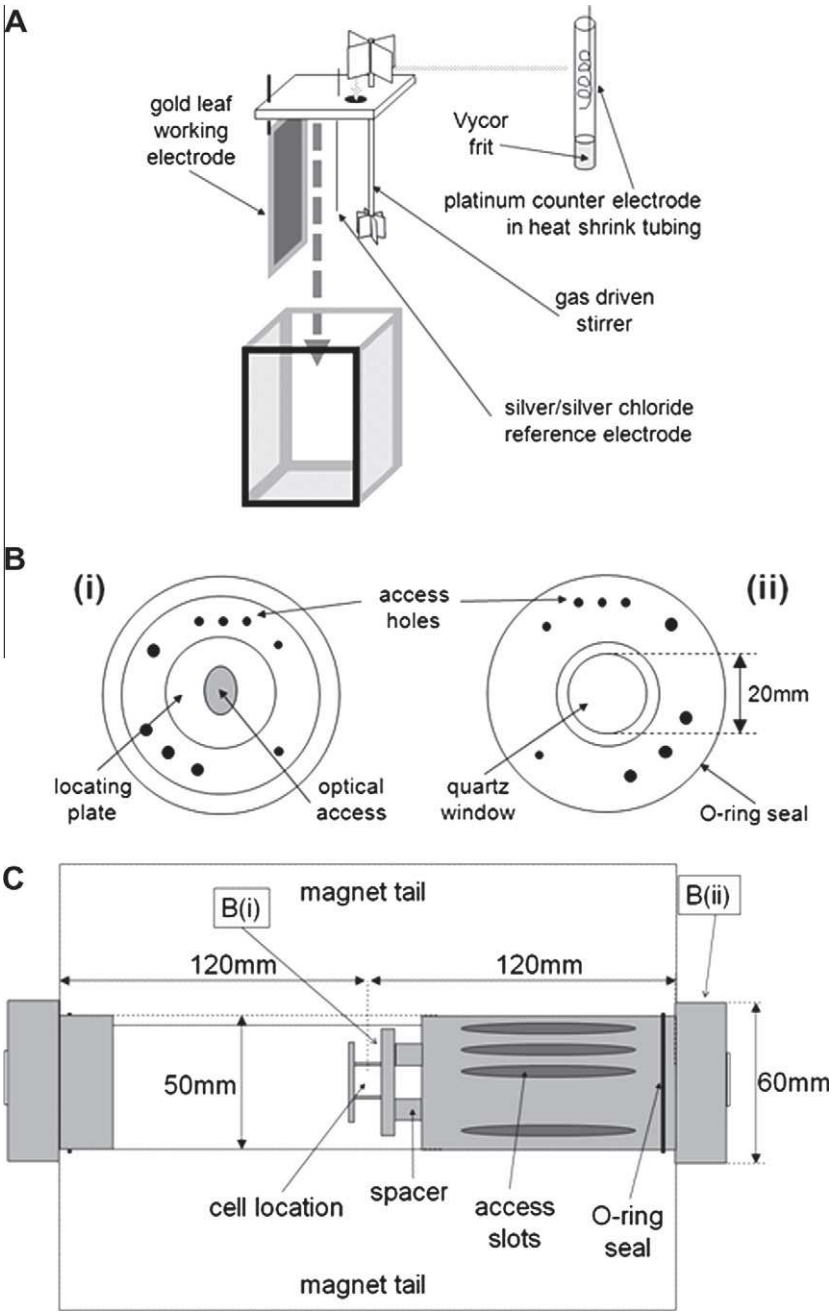


**Fig.1.** Schematic showing the cell holder assembly. (A) Construction of the stirred long-pathlength electrochemical (M)CD cell. (B) Interior face (i) and exterior face (ii) of the bespoke nylon cell holder. (C) Location of the cell holder and plug within the bore of the solenoid.

pathlength, 10 mm width, and 16 mm depth was constructed in-house (Fig. 1A). This comprised a six-bladed polystyrene stirrer of 3 mm diameter attached to a polystyrene rod of 1 mm diameter and 15 mm length. The rod passed through a hole in a Teflon sheet, forming the lid of the cuvette, and was held in place by two Teflon rings, one above the lid and one below it. An impeller was constructed from four pieces of Teflon (6 mm high by 3 mm wide by 1 mm thick) glued to the length of rod that protrudes through the lid. The entire cuvette assembly was transferred into an $N_2$-filled chamber to be filled with anaerobic aqueous solutions of the sample protein. The loaded cuvette was then clamped into a bespoke holder manufactured from nylon by the mechanical workshop of the University of East Anglia (Fig. 1B and C). The cuvette lid and stirring mechanism were affixed by coating the top of the cuvette with a thin layer of vacuum grease.

The cuvette holder, approximately 12 cm in length, allows cuvettes of 0.5–10 mm pathlength to be clamped between circular plates with cut-away sections, allowing optical access. These plates are attached to a cylinder that, when inserted into the solenoid bore, places the cuvette in the center of the magnetic field while maintaining optical access and providing mechanical support for cannulas and electrical connections. Once loaded with cuvette and reagent lines, the holder is transferred from the $N_2$ chamber and placed in the solenoid bore (Fig. 1C). Gas-tight seals are provided by neoprene O-rings; one sits between the cuvette holder and the inside of the bore (Fig. 1C), and the other sits between the outer face of the holder and the quartz window (Fig. 1B). The opposite end of the bore is sealed by a nylon plug with a quartz window (Fig. 1C). The impeller is driven by humidified $N_2$ gas delivered by a cannula threaded through an access channel in

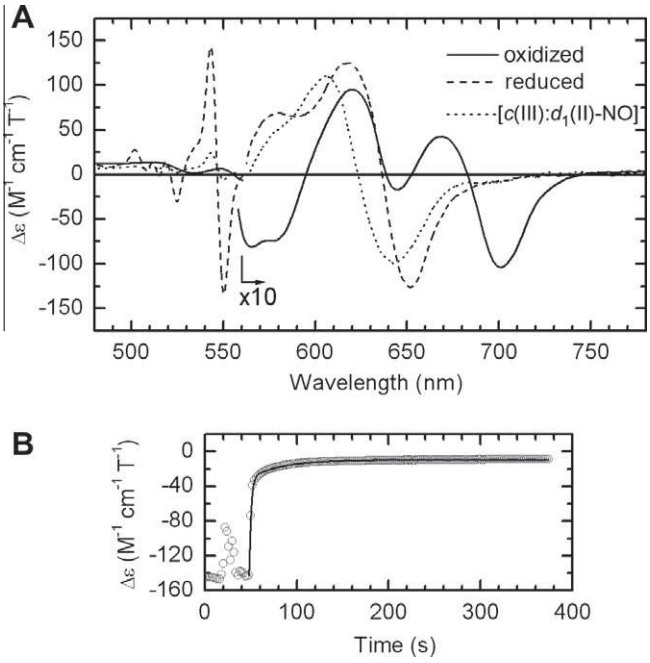


**Fig.2.** In situ reduction and partial reoxidation of cytochrome $cd_1$. Experimental parameters: $cd_1$ monomer concentration, 30 μM; magnetic field, 8 T; pathlength, 1 cm. (A) MCD spectra of $cd_1$ in the oxidized state (—), reduced by sodium dithionite (– – –), and following partial reoxidation with sodium nitrite (. . . . .). (B) Intensity of the 550-nm MCD feature as a function of time following the addition of a molar equivalent of sodium nitrite (1 $NO_2^-$ per $cd_1$ monomer) (○) and the two-component exponential fit (—).

the cuvette holder. A 2-mm hole in the nylon plug provides an exit route for the gas that also serves to maintain anaerobicity within the bore. This arrangement removes the requirement for a gas-tight cuvette lid for anaerobic studies, greatly simplifying the construction. Further access channels in the cuvette holder allow reagent lines and electrical connections to reach the cuvette. Entrances to the access channels are sealed with vacuum grease to minimize oxygen leakage into the bore.

*Assessing the efficiency of reagent injection and stirring mechanisms*

The efficiency of the stirring and reagent injection mechanisms was assessed by in situ reduction and partial reoxidation of the soluble dimeric nitrite reductase, $cd_1$ from *P. pantotrophus,* the MCD and redox properties of which are well understood [32,33]. As purified, the $cd_1$ monomer contains two Fe(III) hemes, *c* and $d_1$. Heme $d_1$ is axially coordinated by tyrosinate ($Tyr^-$) and histidine and exists in a thermal equilibrium between low- and high-spin states [32,34]. The high-spin state gives rise to a characteristic electronic absorption at 702 nm. This appears in the ambient temperature MCD as a bisignate feature with a peak and a trough at approximately 670 and 700 nm, respectively, and is a marker band for the oxidized as-prepared form [32,34]. Importantly, reduced $cd_1$ is rapidly reoxidized by dioxygen, with the return of the 670/700-nm feature. Indeed, $cd_1$ was originally reported for this activity in the belief that it was a cytochrome oxidase [35].

The stirred cuvette containing an anaerobic sample of oxidized $cd_1$ was attached to the cell holder, and this was placed in the bore of the solenoid. The solenoid was energized, and the MCD spectrum was recorded (Fig. 2A, solid line). Approximately two reducing equivalents per monomer were injected into the stirred cell as an aliquot of aqueous buffered sodium dithionite from a preloaded injection line. The MCD spectrum was recorded, and the degree of reduction was calculated. A further small aliquot of dithionite, sufficient to complete the reduction, was added. The resulting MCD spectrum (Fig. 2A, dashed line) is that of fully reduced $cd_1$ [36]. Bands in the 560- to 700-nm region are due to high-spin Fe(II) heme $d_1$ from which the $Tyr^-$ ligand has dissociated. The sharp intense bisignate feature at 544–550 nm arises from low-spin Fe(II) heme *c* [1].

The MCD intensity at 550 nm was then recorded as a function of time (Fig. 2B, open circles). After 50 s, a molar equivalent of nitrite was injected from a second line, triggering an immediate decrease in the MCD signal. The time-dependent loss of intensity could be fitted to the sum of two exponential processes (Fig. 2B, solid line). The faster process was described by an effective first-order rate constant of 0.5 $s^{-1}$ and accounted for loss of the majority of intensity at 550 nm. The second, slower process accounting for smaller loss of intensity was described by an exponential function with a first-order rate constant of 0.028 $s^{-1}$. When no further changes were observed, the visible region MCD spectrum was recorded (Fig. 2A, dotted line). The virtual disappearance of the bisignate 544- to 550-nm feature is consistent with reoxidation of heme *c* to the Fe(III) state. However, levels of the 670/700-nm bisignate feature are negligible; there has been no return to the $Tyr^-$-bound Fe(III) form of heme $d_1$. This is consistent with previous observations that reoxidation of the reduced enzyme by nitrite results in a semireduced form, [*c*(III)/$d_1$(II)-NO], in which heme *c* is predominantly in the Fe(III) state and product is bound to heme $d_1$. Exposure to air leads, within seconds, to the brown color characteristic of the oxidized as-prepared form.

At the pH of this experiment, the reaction of reduced $cd_1$ with nitrite is rapid. In nitrite reductase assays, turnover occurs at approximately $10^2$ $s^{-1}$ [37]. Fourier transform infrared (FTIR) studies show that the initial reaction with nitrite proceeds with $k > 500$ $s^{-1}$ and a subsequent rearrangement occurs in approximately 40 ms [38]. Both steps are extremely rapid compared with the apparent first-order rate measured by the collapse of the 544- to 550-nm MCD feature in this experiment (0.5 $s^{-1}$). Therefore, this figure of 0.5 $s^{-1}$ reports on the rate of reagent mixing in our device; that is, mixing is achieved with a time constant of 2 s. This conclusion is supported by the near identical rate (0.6 $s^{-1}$) measured for the rate of cytochrome *c* reduction by dithionite using the same apparatus (data not shown). The minority slower phase of change at 544–550 nm reports on events specific to $cd_1$ that are being further investigated.

These results demonstrate the efficient basic functioning of the device designed for operation within the solenoid bore. Precise quantities of aqueous reagent, here reducing agent and substrate, can be delivered to the sample as required. The $cd_1$ can be stoichiometrically reduced and subsequently reacted with one molar equivalent of nitrite without reemergence of the 670/700-nm MCD feature, testifying to the fact that the sample, and the reagent delivery tubes, can be maintained and manipulated within a strictly anaerobic environment. The stirring mechanism was operating continuously during acquisition without detriment to the quality of spectra and was shown to completely mix reagents with the sample at a rate of 0.5 $s^{-1}$.

*Incorporation of a stirred electrochemical cell*

Minor modification of the cuvette lid described allowed a three-electrode cell configuration with physical separation of counter and working electrodes (Fig. 1A). A coil of platinum wire forms the counter electrode and is separated from the sample by a Vycor frit enclosed in heat-shrink tubing and filled with buffer–electrolyte solution. This was immersed in the sample via a hole in the lid positioned such that the assembly does not impinge on the light path. Additional holes bored through the lid allowed a silver/silver chloride reference electrode and working electrode to be

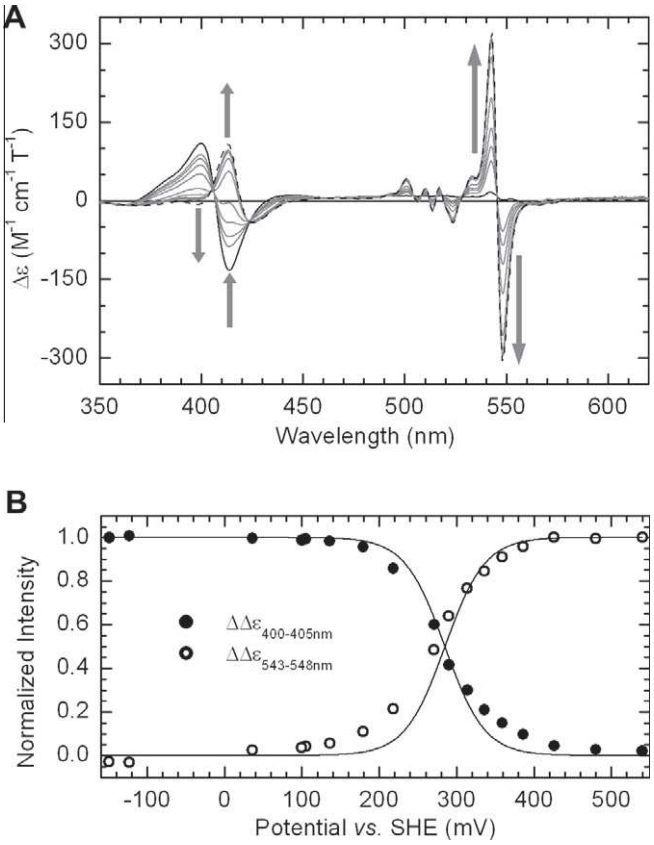


**Fig.3.** Potentiometric titrations of cytochrome *c*, in the stirred electrochemical cell, monitored by MCD spectroscopy. Experimental parameters: protein concentration, 6 μM; buffer/electrolyte, 20 mM Hepes and 50 mM KCl (pH 7.4); magnetic field, 8 T; pathlength, 1 cm. (A) MCD spectra for sample equilibrated at a range of potentials between the extremes of +540 mV (—) and −149 mV (– – –). Arrows indicate the change in intensity on reduction. (B) Plots versus potential of: the variation in peak-to-trough intensity of the bisignate MCD feature at 545 nm (○), the intensity of the 400-nm MCD feature measured as $\Delta\Delta\varepsilon_{400-405\ nm}$ (●), and the behavior predicted by the Nernst equation for a single one-electron center with a midpoint potential of $E_m$ = +280 mV (—).

connected to wires leading to a potentiostat. The working electrode was a gold foil "flag" of approximate dimensions 9 × 9 × 0.5 mm, arranged such that the shortest dimension lay parallel to the transparent faces of the cuvette. Both the reference and working electrodes were positioned out of the light path.

*Testing of electrochemical cell by potentiometric titrations of heme and copper centers: cytochrome c and Paz*

The MCD of a solution of cytochrome *c* initially poised at +540 mV was dominated by a bisignate feature centered at 407 nm, typical of low-spin Fe(III) heme (Fig. 3A, solid black line). On equilibrating the sample at a series of increasingly negative potentials down to −149 mV, this was gradually replaced by an asymmetric bisignate feature at 419 nm and a sharp bisignate at 545 nm that together constitute the MCD of low-spin Fe(II) heme. Simple interconversion was indicated by isosbestic points at 405 and 424 nm. Full reduction of the sample was confirmed by the relative intensities of the 400- and 413-nm peaks at high and low potentials, respectively [25]. The final spectrum of the reduced form is shown as the dashed black line in Fig. 3. The variation in peak-to-trough intensity of the 545-nm band with applied potential (Fig. 3B, open circles) was well described by the Nernst equation for a one-electron process with a midpoint potential of +280 mV versus the standard hydrogen electrode (SHE). The same midpoint potential described equally well the spectral changes $\Delta\Delta\varepsilon_{(400-405\ nm)}$, the diminishing Fe(III) peak referenced to the isosbestic point (Fig. 3B, solid circles). This midpoint potential is in good agreement with values reported previously [25,39].

Paz of *P. pantotrophus* was chosen to investigate the suitability of the apparatus to monitor, by RT MCD, the potentiometry of cofactors other than heme. Paz contains a single type I "blue copper" center, a cofactor involved in a variety of biological electron transfer processes. The characteristic blue color is a result of charge transfer transitions from a coordinating cysteinate sulfur atom to the $d^9$ Cu(II) ion [40]. One-electron reduction to the Cu(I) ($d^{10}$) precludes charge transfer and bleaches the color, abolishing both CD and MCD. Ambient temperature CD and MCD of Paz, recorded across the visible region (not shown), were consistent with previous reports for blue copper centers in that the MCD is significantly lower in intensity than the natural CD [41]. The CD results from chirality of ligand conformation at Cu(II), but the orbital angular momentum required for MCD is almost completely quenched. This situation is reversed for the high-symmetry achiral heme chromophore, which relies for its weak CD on a small degree of chirality imposed by the surrounding amino acid side chains. But porphyrin-excited states involved in electronic transitions possess significant orbital angular momentum, leading to intense MCD. Therefore, in terms of resolving optical bands, MCD offers no advantages; the oxidation state of a type I copper center is more easily monitored using the natural CD. This spectroscopic contrast between heme and type I copper potentially allows discrimination in samples containing both centers. The MCD and absorbance of heme is such that it would render spectra of type I copper impossible to detect in such samples containing equimolar levels. Therefore, the combined in situ use of CD and MCD in electrochemical titrations may provide an efficient method of deconvoluting spectral responses from a variety of multicenter enzymes that contain both copper and heme [42–44]. The disparity between CD and MCD intensities of heme and blue copper centers is also observed between heme and the dinuclear $Cu_A$ site found in the heme copper oxidases and nitrous oxide reductase [45–47].

The MCD and CD spectra of a sample containing approximately equimolar cytochrome *c* and Paz were measured with the sample fully oxidized and fully reduced. In both oxidation states, the MCD observed was essentially that of cytochrome *c*, as already shown in Fig. 3; the response from Paz is too weak to be observed in the presence of intense heme bands. CD spectra of the oxidized and reduced forms of the mixture are shown in Fig. 4A. The CD of the oxidized mixture is now predominantly that of Cu(II) Paz, with minimal contributions from cytochrome *c* near 410 nm. In a sample containing equimolar heme and type I copper chromophores, overall concentration will be limited by the intense absorption of the former. The ability of the CD spectrum to probe effectively the redox properties of type I copper at these concentrations was demonstrated by using CD to monitor a potentiometric titration of Paz. Titrations were performed in both the reductive and oxidative directions, confirming that loss of CD intensity on reduction was not due to denaturation of the type I site. CD spectra recorded during the reductive phase are shown in Fig. 4B. A plot of peak-to-trough intensity $\Delta\Delta\varepsilon_{(395-465\ nm)}$ versus potential was well described by the Nernst equation for an $n$ = 1 center with a midpoint potential of +265 mV versus SHE (Fig. 4C) and again was in good agreement with values reported previously [48].

Equilibration of both cytochrome *c* and Paz with applied potential occurred within 20–60 min. This compares favorably with the equilibration times of the previous generation of electrochemical MCD cells and is sufficient to allow the measurement of a potentiometric titration in both the oxidative and reductive directions in a single day despite the order of magnitude increase in pathlength.

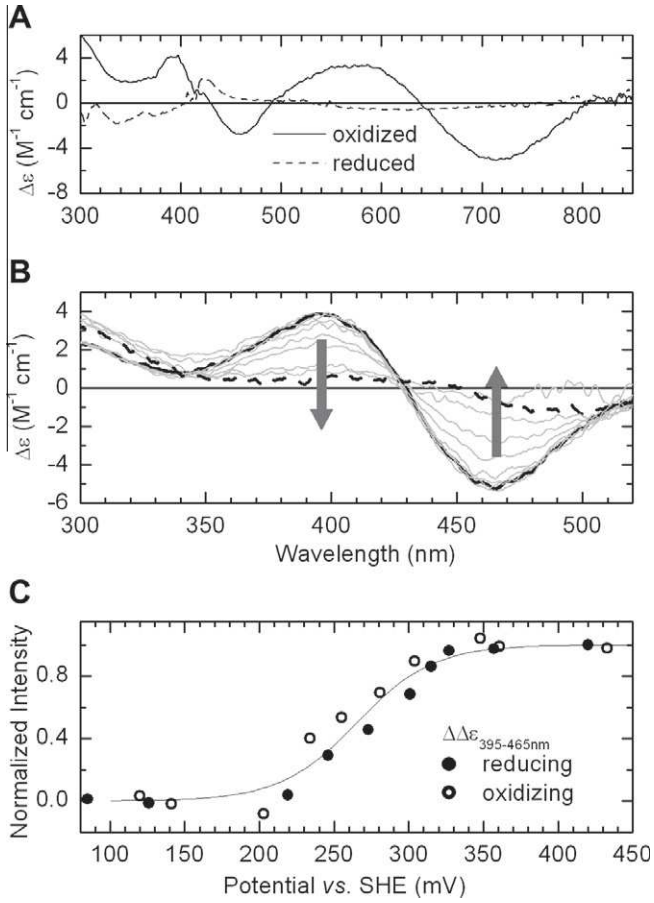


**Fig.4.** (A) CD spectra for an equimolar mixture (30 μM each) of cytochrome *c* and Paz in the fully reduced state (……) and fully oxidized state (—). Experimental parameters: pathlength, 1 cm. (B) Potentiometric titrations of Paz, in the stirred electrochemical cell, monitored by CD spectroscopy. Experimental parameters: protein concentration, 50 μM; buffer/electrolyte, 50 μM concentration in 50 mM potassium phosphate and 50 mM KCl (pH 8.0); pathlength, 1 cm. (B) CD spectra for sample equilibrated at a range of potentials between the extremes of +420 mV (—) and +85 mV (– – –). Arrows indicate the change in intensity on reduction. (C) Plots versus potential of the variation in CD intensity $\Delta\Delta\varepsilon_{395-465\ nm}$ for the reductive titration (●) and oxidative titration (○) and the behavior predicted by the Nernst equation for a single one-electron center with a midpoint potential of $E_m$ = +265 mV (—).

## Discussion

We were able to monitor time-resolved MCD signals resulting from in situ chemical manipulation of a metalloprotein sample for the first time. This was achieved by developing a cuvette-positioning apparatus that allows reagent injection and sample mixing within the 50-mm-diameter bore of an energized superconducting magnet. The injection system is capable of accurately delivering small volumes (0.5 μl) of reagent into the sample (typically 1300 μl). Thus, dilution is minimal, a critical feature for sequential or repeated reagent additions.

Data acquisition may be simultaneous with reagent injection. The frequency of data collection is determined by the spectrometer and corresponds to a maximum of 10 $s^{-1}$ when MCD is recorded at a single wavelength with the Jasco J-810 spectropolarimeter used in these studies. Thus, the configuration we report allows the first data point to be measured 0.1 s after reagent injection, although mixing of sample and reagent clearly remains incomplete at this point. Nevertheless, an apparent first-order rate constant of 0.5 $s^{-1}$ for mixing of sample and injected reagent means that homogeneity of greater than 99% for a 1300-μl sample is achieved within 15 s. Compared with previous methods for accessing time-resolved MCD data by a freeze–quench approach, this represents an improvement of approximately two orders of magnitude in the "dead time" prior to which the first representative data point cannot be collected. An additional advantage of the method reported here is that a single sample allows complete resolution of a reaction time course with high fidelity. Finally, and not insignificantly given that many metalloproteins react with oxygen in reactions that mask the reactivity of interest, it is notable that all of this is achieved within a rigorously oxygen-free environment.

The increased volume and stirring capabilities of the newly developed MCD cuvettes offer two immediate benefits to in situ electrochemical sample manipulation. In MOTTLE cells, the electrode is placed in the light path to ensure minimal times for equilibration of the sample by diffusion. With the new cuvettes, there is no longer a requirement for optically transparent electrode materials because the electrode can be placed to one side of the light path. Thus, opaque and high surface area working electrodes can be employed, including those made of graphite or glassy carbon; these offer access to a wider potential window than metal electrodes. Equilibration of the sample and applied potential in the new cuvettes occurs within a timeframe similar to that achieved by MOTTLE cells. However, the new cuvettes allow redox events at the working electrode to be physically separated from the compensating events occurring at the counter electrode that are required to support current flow. This has the significant advantage of minimizing the opportunity for processes at the counter electrode to inadvertently introduce additional reactants into the sample.

Using the rapid reaction of reduced cytochrome $cd_1$ with nitrite, we measured a slower apparent rate constant of 0.5 $s^{-1}$, thereby defining the efficiency of the mixing mechanism. In principle, metalloprotein events occurring at comparable, or slower, rates will be amenable to study by the reagent-triggered, time-resolved MCD approach presented here. With the ability of the new cuvettes to boost MCD intensity to the extent that centers with weak characteristic MCD signatures such as type I copper are now amenable to study, there are exciting opportunities for applying MCD to study reagent-triggered reactions in a variety of metalloproteins. Developments in these areas will be reported in future articles. Finally, we note that the enhanced capabilities of the cuvettes reported here can also be employed for MCD of heme proteins adsorbed on mesoporous nanocrystalline $SnO_2$ electrodes [49]. Thus, the introduction of substrate into a stirred solution contacting an adsorbed electroactive protein film offers the prospect of resolving the oxidation, ligation, and spin states of the predominant enzyme form(s) present during steady-state catalysis at defined electrochemical potential. Such experiments are likely to provide valuable insight into the variation of catalytic rate-defining events with applied potential, an area where much remains to be elucidated [50].

## Acknowledgment

We thank the Biotechnology and Biological Sciences Research Council (BBSRC) for financial support through grant BB/G024758/1.

## References

[1] M.R. Cheesman, C. Greenwood, A.J. Thomson, Magnetic circular dichroism of hemoproteins, Adv. Inorg. Chem. 36 (1991) 201–255.
[2] M.R. Cheesman, V.S. Oganesyan, N.J. Watmough, C.S. Butler, A.J. Thomson, The nature of the exchange coupling between high-spin Fe(III) heme $o_3$ and $Cu_B$(II) in *Escherichia coli* quinol oxidase, cytochrome $bo_3$: MCD and EPR studies, J. Am. Chem. Soc. 126 (2004) 4157–4166.
[3] S.J. Field, L. Prior, M.D. Roldan, M.R. Cheesman, A.J. Thomson, S. Spiro, J.N. Butt, N.J. Watmough, D.J. Richardson, Spectral properties of bacterial nitric-oxide

reductase: resolution of pH-dependent forms of the active site heme $b_3$, J. Biol. Chem. 277 (2002) 20146–20150.
[4] E.I. Solomon, E.G. Pavel, K.E. Loeb, C. Campochiaro, Magnetic circular dichroism spectroscopy as a probe of the geometric and electronic structure of non-heme ferrous enzymes, Coord. Chem. Rev. 144 (1995) 369–460.
[5] K. Rupnik, Y.-L. Hu, A.W. Fay, M.W. Ribbe, B.J. Hales, Variable-temperature variable-field magnetic circular dichroism spectroscopic study of NifEN-bound precursor and FeMoco, J. Biol. Inorg. Chem. 16 (2011) 325–332.
[6] E.M. Walters, M.K. Johnson, in: Ferredoxin:thioredoxin Reductase: disulfide reduction catalyzed via novel site-specific [4Fe–4S] cluster chemistry, Photosynth. Res. 79 (2004) 249–264.
[7] P. Hänzelmann, H.L. Hernández, C. Menzel, R. García-Serres, B.H. Huynh, M.K. Johnson, R.R. Mendel, H. Schindelin, Characterization of MOCS1A an oxygen-sensitive iron–sulfur protein involved in human molybdenum cofactor biosynthesis, J. Biol. Chem. 279 (2004) 34721–34732.
[8] G. Mitou, C. Higgins, P. Wittung-Stafshede, R.C. Conover, A.D. Smith, M.K. Johnson, J. Gaillard, A. Stubna, E. Münck, J. Meyer, An Isc-type extremely thermostable [2Fe–2S] ferredoxin from *Aquifex aeolicus:* biochemical spectroscopic and unfolding studies, Biochemistry 42 (2003) 1354–1364.
[9] K.S. Hadler, N. Mitić, S. H-C. Yip, L.R. Gahan, D.L. Ollis, G. Schenk, J.A. Larrabee, Electronic structure analysis of the dinuclear metal center in the bioremediator glycerophosphodiesterase (GpdQ) from *Enterobacter aerogenes*, Inorg. Chem. 49 (2010) 2727–2734.
[10] J.A. Larrabee, C.M. Alessi, E.T. Asiedu, J.O. Cook, K.R. Hoerning, L.J. Klingler, G.S. Okin, S.G. Santee, T.L. Volkert, Magnetic circular dichroism spectroscopy as a probe of geometric and electronic structure of cobalt(II)-substituted proteins: ground-state zero-field splitting as a coordination number indicator, J. Am. Chem. Soc. 119 (1997) 4182–4196.
[11] E.C. Duin, L. Signor, R. Piskorski, F. Mahlert, M.D. Clay, M. Goenrich, R.K. Thauer, B. Jaun, M.K. Johnson, Spectroscopic investigation of the nickel-containing porphinoid cofactor F430: comparison of the free cofactor in the +1, +2, and +3 oxidation states with the cofactor bound to methyl-coenzyme M reductase in the silent, red, and ox forms, J. Biol. Inorg. Chem. 9 (2004) 563–576.
[12] M.K. Johnson, I.C. Zambrano, M.H. Czechowski, H.D. Peck Jr., D.V. DerVartanian, J. LeGall, Low temperature magnetic circular dichroism spectroscopy as a probe for the optical transitions of paramagnetic nickel in hydrogenase, Biochem. Biophys. Res. Commun. 128 (1985) 220–225.
[13] J.L. Craft, P.W. Ludden, T.C. Brunold, Spectroscopic studies of nickel-deficient carbon monoxide dehydrogenase from *Rhodospirillum rubrum*: nature of the iron–sulfur clusters, Biochemistry 41 (2002) 1681–1688.
[14] T. Rasmussen, B.C. Berks, J.N. Butt, A.J. Thomson, Multiple forms of the catalytic centre $Cu_Z$ in the enzyme nitrous oxide reductase from *Paracoccus pantotrophus*, Biochem. J. 364 (2002) 807–815.
[15] L. Quintanar, J. Yoon, C.P. Aznar, A.E. Palmer, K.K. Andersson, R.D. Britt, E.I. Solomon, Spectroscopic and electronic structure studies of the trinuclear Cu cluster active site of the multicopper oxidase laccase: nature of its coordination unsaturation, J. Am. Chem. Soc. 127 (2005) 13832–13845.
[16] A.J. Thomson, M.R. Cheesman, S.J. George, Variable-temperature magnetic circular dichroism, Methods Enzymol. 226 (1993) 199–232.
[17] M.R. Cheesman, F.A. Walker, Low-temperature MCD studies of low-spin ferric complexes of tetramesitylporphyrinate: evidence for the novel $(d_{xz},d_{yz})^4(d_{xy})^1$ ground state which models the spectroscopic properties of heme d, J. Am. Chem. Soc. 118 (1996) 7373–7380.
[18] M.K. Johnson, A.J. Thomson, A.E. Robinson, K.K. Rao, D.O. Hall, Low-temperature magnetic circular dichroism spectra and magnetization curves of 4Fe clusters in iron–sulfur proteins from *Chromatium* and *Clostridium pasteurianum*, Biochim. Biophys. Acta 667 (1981) 433–451.
[19] A.J. Thomson, A.E. Robinson, M.K. Johnson, J.J.G. Moura, I. Moura, A.V. Xavier, J. LeGall, The 3-iron cluster in a ferredoxin from *Desulfovibrio gigas*: a low-temperature magnetic circular dichroism study, Biochim. Biophys. Acta 670 (1981) 93–100.
[20] M.K. Johnson, R.E. Duderstadt, E.C. Duina, Biological and synthetic $[Fe_3S_4]$ clusters, Adv. Inorg. Chem. 47 (1999) 1–82.
[21] P.M.A. Gadsby, A.J. Thomson, Assignment of the axial ligands of ferric ion in low-spin hemoproteins by near-infrared magnetic circular dichroism and electron paramagnetic resonance spectroscopy, J. Am. Chem. Soc. 112 (1990) 5003–5011.
[22] R.M. Jones, F.E. Inscore, R. Hille, M.L. Kirk, Freeze–quench magnetic circular dichroism spectroscopic study of the "very rapid" intermediate in xanthine oxidase, Inorg. Chem. 38 (1999) 4963–4970.
[23] J.W.A. Allen, M.R. Cheesman, C.W. Higham, S.J. Ferguson, N.J. Watmough, A novel conformer of oxidized *Paracoccus pantotrophus* cytochrome $cd_1$ observed by freeze–quench NIR–MCD spectroscopy, Biochem. Biophys. Res. Commun. 279 (2000) 674–677.
[24] N. Mitić, M.D. Clay, L. Saleh, J.M. Bollinger Jr., E.I. Solomon, Spectroscopic and electronic structure studies of intermediate X in ribonucleotide reductase R2 and two variants: a description of the $Fe^{IV}$–oxo bond in the $Fe^{III}$–O–$Fe^{IV}$ dimer, J. Am. Chem. Soc. 129 (2007) 9049–9065.
[25] S.J. Marritt, J.H. van Wonderen, M.R. Cheesman, J.N. Butt, Magnetic circular dichroism of hemoproteins with in situ control of electrochemical potential: MOTTLE, Anal. Biochem. 359 (2006) 79–83.
[26] S.J. Marritt, G.L. Kemp, L. Xiaoe, J.R. Durrant, M.R. Cheesman, J.N. Butt, Spectroelectrochemical characterization of a pentaheme cytochrome in solution and as electrocatalytically active films on nanocrystalline metal–oxide electrodes, J. Am. Chem. Soc. 130 (2008) 8588–8589.
[27] L. Male, S.J. Marritt, B.C. Berks, M.R. Cheesman, J.H. van Wonderen, S.J. George, J.N. Butt, Protein voltammetry and spectroscopy: integrating approaches, Theor. Chem. Account. 19 (2008) 107–111.
[28] J.W.B. Moir, D. Baratta, D.J. Richardson, S.J. Ferguson, The purification of a $cd_1$-type nitrite reductase from, and the absence of a copper-type nitrite reductase from, the aerobic denitrifier *Thiosphaera pantotropha*: the role of pseudoazurin as an electron donor, Eur. J. Biochem. 212 (1993) 377–385.
[29] K. Kobayashi, A. Koppenhofer, S.J. Ferguson, S. Tagawa, Pulse radiolysis studies on cytochrome $cd_1$ nitrite reductase from *Thiosphaera pantotropha*: evidence for a fast intramolecular electron transfer from *c*-heme to $d_1$-heme, Biochemistry 36 (1997) 13611–13616.
[30] B.F. van Gelder, E.C. Slater, The extinction coefficient of cytochrome *c*, Biochim. Biophys. Acta 58 (1962) 593–595.
[31] S.R. Pauleta, F. Guerlesquin, C.F. Goodhew, B. Devreese, J. van Beeumen, A.S. Pereira, I. Moura, G.W. Pettigrew, *Paracoccus pantotrophus* pseudoazurin is an electron donor to cytochrome *c* peroxidase, Biochemistry 43 (2004) 11214–11225.
[32] M.R. Cheesman, S.J. Ferguson, J.W.B. Moir, D.J. Richardson, W.G. Zumft, A.J. Thomson, Two enzymes with a common function but different heme ligands in the forms as isolated: optical and magnetic properties of the heme groups in the oxidized forms of nitrite reductase, cytochrome $cd_1$, from *Pseudomonas stutzeri* and *Thiosphaera pantotropha*, Biochemistry 36 (1997) 16267–16276.
[33] A. Koppenhofer, K.L. Turner, J.W.A. Allen, S.K. Chapman, S.J. Ferguson, Cytochrome $cd_1$ from *Parococcus pantotrophus* exhibits kinetically gated, conformationally dependent, highly cooperative two-electron redox behavior, Biochemistry 39 (2000) 4243–4249.
[34] V. Fulop, J.W.B. Moir, S.J. Ferguson, J. Hajdu, The anatomy of a bifunctional enzyme-structural basis for reduction of oxygen to water and synthesis of nitric oxide by cytochrome $cd_1$, Cell 81 (1995) 369–377.
[35] T. Horio, T. Higashi, K. Okunuki, H. Matsubara, T. Yamanaka, Purification and properties of cytochrome oxidase from *Pseudomonas aeruginosa*, J. Biol. Chem. 236 (1961) 944–951.
[36] L.E. Vickery, G. Palmer, D.C. Wharton, Heme *c*-heme $d_1$ interaction in *Pseudomonas* cytochrome oxidase (nitrite reductase): reappraisal of spectroscopic evidence, Biochem. Biophys. Res. Commun. 80 (1978) 458–463.
[37] C.D. Richter, J.W.A. Allen, C.W. Higham, A. Koppenhofer, R.S. Zajicek, N.J. Watmough, S.J. Ferguson, Cytochrome $cd_1$, reductive activation and kinetic analysis of a multifunctional respiratory enzyme, J. Biol. Chem. 277 (2002) 3093–3100.
[38] S.J. George, J.W.A. Allen, S.J. Ferguson, R.N.F. Thorneley, Time-resolved infrared spectroscopy reveals a stable ferric heme–NO intermediate in the reaction of *Paracoccus pantotrophus* cytochrome $cd_1$ nitrite reductase with nitrite, J. Biol. Chem. 275 (2000) 33231–33237.
[39] F.A. Armstrong, A.O. Hill, N.J. Walton, Direct electrochemistry of redox proteins, Acc. Chem. Res. 21 (1988) 407–413.
[40] E.I. Solomon, R.G. Hadt, Recent advances in understanding blue copper proteins, Coord. Chem. Rev. 255 (2011) 744–789.
[41] E.I. Solomon, J.W. Hare, D.M. Dooley, J.H. Dawson, P.J. Stephens, Spectroscopic studies of stellacyanin, plastocyanin, and azurin: electronic structure of the blue copper sites, J. Am. Chem. Soc. 102 (1980) 168–178.
[42] J. Abramson, M. Svensson-Ek, B. Byrne, S. Iwata, Structure of cytochrome *c* oxidase: a comparison of the bacterial and mitochondrial enzymes, Biochim. Biophys. Acta 1544 (2001) 1–9.
[43] M.J.F. Suharti, J.F. Strampraad, Schröder S. de Vries, A novel copper-A containing menaquinol NO reductase from *Bacillus azotoformans*, Biochemistry 40 (2001) 2632–2639.
[44] J. Simon, O. Einsle, P.M.H. Kroneck, W.G. Zumft, The unprecedented nos gene cluster of *Wolinella succinogenes* encodes a novel respiratory electron transfer pathway to cytochrome *c* nitrous oxide reductase, FEBS Lett. 569 (2004) 7–12.
[45] J.A. Farrar, N. Neese, P. Lappalainen, P.M.H. Kroneck, M. Saraste, W.G. Zumft, A.J. Thomson, The electronic structure of $Cu_A$: a novel mixed-valence dinuclear copper electron-transfer center, J. Am. Chem. Soc. 118 (1996) 11501–11514.
[46] D.M. Dooley, J.M.A. McGuirl, A.C. Rosenzweig, J.A. Landin, R.A. Scott, W.G. Zumft, F. Devlin, P.J. Stephens, Spectroscopic studies of the copper sites in wild-type *Pseudomonas stutzeri* $N_2O$ reductase and in an inactive protein isolated from a mutant deficient in copper-site biosynthesis, Inorg. Chem. 30 (1991) 3006–3011.
[47] D.R. Gamelin, D.W. Randall, M.T. Hay, R.P. Houser, T.C. Mulder, G.W. Canters, S. de Vries, W.B. Tolman, Y. Lu, E.I. Solomon, Spectroscopy of mixed-valence $Cu_A$-type centers: ligand-field control of ground-state properties related to electron transfer, J. Am. Chem. Soc. 120 (1998) 5246–5263.
[48] P.M. Paes de Sousa, S.R. Pauleta, M.L. Simões Gonçalves, G.W. Pettigrew, I. Moura, M.M. Correia dos Santos, J.J.G. Moura, Mediated catalysis of *Paracoccus pantotrophus* cytochrome *c* peroxidase by *P. pantotrophus pseudoazurin*: kinetics of intermolecular electron transfer, J. Biol. Inorg. Chem. 12 (2007) 691–698.
[49] G.L. Kemp, S.J. Marritt, L. Xiaoe, J.R. '-Durrant, M.R. Cheesman, J.N. Butt, Opportunities for mesoporous nanocrystalline $SnO_2$ electrodes in kinetic and catalytic analyses of redox proteins, Biochem. Soc. Trans. 37 (2009) 368–372.
[50] A.J. Gates, G.L. Kemp, C.Y. To, J. Mann, S.J. Marritt, A.G. Mayes, D.J. Richardson, J.N. Butt, The relationship between redox enzyme activity and electrochemical potential: cellular and mechanistic implications from protein film electrochemistry, Phys. Chem. Chem. Phys. 13 (2011) 7720–7731.